Theoretical study of structural, electronic, optical and Thermodynamic properties of AlP, InP and AlAs compounds

ALI BENTOUAF[*,a], TARIK OUAHRANI[b], MOHAMMED AMERI[a], REZKI MEBSOUT[c], DJELLOUL HACHEMANE[a].
[a]*Laboratory physico-chemistry of advanced materials, University of Djillali Liabes, BP 89, Sidi-Bel Abbes, 22000, Algeria*
[b]*Laboratoire de Physique Théorique, Université de Tlemcen, 13000 Tlemcen, Algeria.*
[c]*Laboratoire de Modélisation et de Simulation en Sciences des Matériaux Université Djillali Liabès, Sidi Bel-Abbes, Algerie*

A theoretical study of structural, electronic, optical and thermodynamic properties of AlP, InP and AlAs compounds is presented; using the full -potential linear muffin-tin orbital (FP-LMTO) method within density functional theory (DFT). In this approach, the generalized gradient approximation (GGA) was used for the exchange-correlation potential calculation. The groundstate properties are determined for the bulk materials (AlP, InP and AlAs) in cubic phase. Quantities such as the lattice constants and bulk modulus of interest are calculated. Detailed comparisons are made with published experimental and theoretical data and show generally good agreement.The calculated lattice constants scale linearly with composition (Vegard's law). The microscopic origins of the gap bowing were explained by using the approach of Zunger and co-workers. In addition, to (FP-LMTO) method, the composition dependence of the refractive index was studied by Reedy and Nazeer model. The thermodynamic stability of these alloys was investigated by calculating the excess enthalpy of mixing ΔH_m as well as the phase diagram.

(Received January 27, 2013; accepted September 18, 2013)

Keywords: FP-LMTO, DFT, Optical properties, Critical temperature

1. Introduction

Recently, III–V zinc blende semiconductors compounds occupya privileged position in the domain of materials science. The reason for this is the prediction ofnew materials, which were previously inaccessible and impossible to study. Among them, the compounds AlAs, InP and AlP are concerned in this paper. AlAs is one of the most important electronic and optoelectronic materials because of its frequent incorporation into GaAs-based heterostructures[1,2]. AlP, with the largest direct gap of the III–V compound semiconductors, is undoubtedly the most ''exotic'' and least studied [1]. However, in recent years, it is attracted special attention to its incorporation in the AlAs/AlP and GaP/AlP-based heterostructures. AlAs/AlPsuperlattices are attractive due to their various electronic properties advantageous, these semiconductors are introduced in most optoelectronic devices, in the field of high-speed electronics, and they are widely used as substrates for the design of ternary and quaternary because they are expected to become direct band gap materials[3].

InP is also an established technology platform for making active optical components such as laser and photo detectors. Its energy band gap can be tuned between 920 and 1650 nm, which makes it ideal for optical communication applications.

InP is also used to produce mostly standalone active components, while devices such as couplers and waveguides tend to be formed from different material platforms optimized for each application. This multi-functionality makes InP an excellent platform for monolithic integration.

Recently, there have been numerous calculations [4-6]of the structural, electronic and optical properties of compounds of these compounds using the method FP-LAPW coupled with thelocal density approximation (LDA) [7] of the exchange-correlation energy to calculate electronic and optical properties, respectively, to our knowledge there are few reports that had used the full potential calculation FP-LAPW to calculate the electronic, structural and optical properties for those compounds.

In the present work, we have aimed to combine AlP, InP and AlAs compounds having different structural and electronic properties in order to obtain new materials, $AlAs_{1-x}P_x$ and $Al_xIn_{1-x}P$ternary alloys with intermediate properties. However, to the best of our knowledge, no experimental or theoretical investigations of our alloys have been appeared in the literature. The present work study the structural, electronic, optical, and thermodynamic properties of these alloys by using a full-potential linear muffin-tin orbital (FP-LMTO) method. The physical origins of gap bowing are calculated following the approach of Zunger and co-workers [8].

The paper is divided in three parts. In Section 2, we briefly describe the computational techniques used in this study. We present the theoretical results and discussion concerning the structural, electronic, optical and thermodynamic properties in Section 3. Finally, in Section 4 we summarize the main conclusions of our work.

2. Computational details

The calculations reported here were carried out using the ab-initio full-potential linear muffin-tin orbital (FP-LMTO) method as implemented in the Lmtart code[9-11]. The exchange and correlation potential was calculated using the gradient generalized approximation (GGA)[12]. This is an improved method compared to previous (LMTO) methods. The FP-LMTO method treats muffin-tin spheres and interstitial regions on the same footing, leading to improvements in the precision of the eingen-values. At the same time, the FP-LMTO method, in which the space is divided into an interstitial regions (IR) and non overlapping muffin-tin spheres (MTS) surrounding the atomic sites, uses a more complete basis than its predecessors. In the IR regions, the basis functions are represented by Fourier series. Inside the MTS spheres, the basis functions are represented in terms of numerical solutions of the radial Schrödinger equation for the spherical part of the potential multiplied by spherical harmonics. The charge density and the potential are represented inside the MTS by spherical harmonics up to l_{max} = 6. The integrals over the Brillouin zone are performed up to 55 special k-points for binary com-pounds and 27 special k-points for the alloys in the irreducible Brillouin zone (IBZ), using the Blöchl's modified tetrahedron method[13]. The self-consistent calculations are considered to be converged when the total energy of the system is stable within 10^{-5} Ry. In order to avoid the overlap of atomic spheres the MTS radius for each atomic position is taken to be different for each case. Both the plane waves cut-off are varied to ensure the total energy convergence. The values of the sphere radii (MTS), number of plane waves (NPLW).

3. Results and discussion

3.1. Structural properties

To investigate the structural properties of AlP, AlAs and InP compounds and their alloys in the cubic structure, we have started our FP-LMTO calculation with the zinc-blende structure and let the calculation forces to move the atoms to their equilibrium positions. We have chosen the basic cubic cell as the unit cell. In the unit cell there are four C anions , three A and one B, two A and two B, and one A and three B cations, respectively, for x = 0.25, 0.50 and 0.75. For the considered structures, we perform the structural optimization by calculating the total energies for different volumes around the equilibrium cell volume V_0 of the binary AlP, InP compound and their alloy. The calculated total energies are fitted to the Murnaghan's equation of state [14] to determine the ground state properties such as the equilibrium lattice constant a, and the bulk modulus B. The equilibrium structural properties such as the lattice constants and bulk modulus were obtained for both binary compounds and their alloys, the results are given in Table1. Considering the general trend that GGA usually overestimates the lattice parameters[15], our GGA results of binary compounds are in good agreement with the experimental and other calculated values. Figs. 1 and 2, show the variation of the calculated equilibrium lattice constants and the bulk modulus versus concentration x for $Al_xIn_{1-x}P$ and $AlAs_{1-x}P_x$. Our calculated lattice parameters at different compositions of $Al_xIn_{1-x}P$ alloy were found to vary almost linearly following Vegard's law [16] with a marginal upward bowing parameter equal to -0,07143 Å. The physical origin of this marginal bowing parameter should be mainly due to the weak mismatches of the lattice constants of InP and AlP compounds. The lattice parameter bowing for $AlAs_{1-x}P_x$ alloy has been found to be -0,2208Å. This is relatively a large value compared to the corresponding one of $Al_xIn_{1-x}P$ alloy, roots in the significant mismatch of the lattice constants of AlP with respect to the other binary compounds. The composition dependence of the bulk modulus is compared with the results predicted by linear concentration dependence (LCD). A significant deviation from LCD, with downward bowings equal to +21,925 and +15,933GPa for $Al_xIn_{1-x}P$ and $AlAs_{1-x}P_x$alloys, respectively, was observed in Fig. 2 a and b. This deviation is mainly due to mismatch of the bulk modulus of binary compounds. It is clearly seen that the bulk modulus decreases by increasing the III-P and Al-V atomic number for $Al_xIn_{1-x}P$ and $AlAs_{1-x}P_x$ respectively. Hence, we conclude that AlAs is more compressible compared to the other binary compounds.

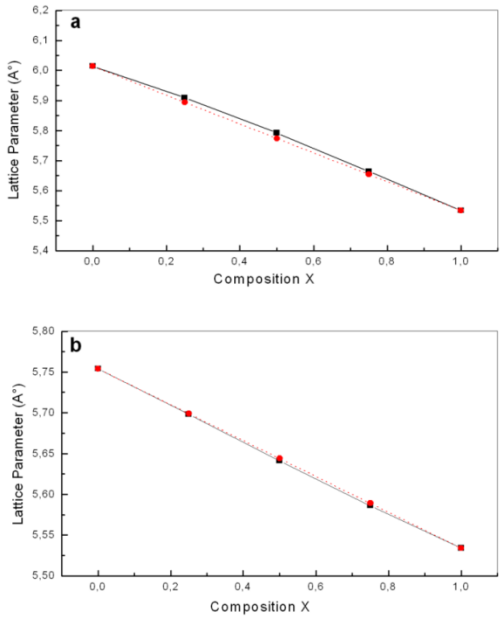

Fig. 1. Composition dependence of the calculated lattice constants (solid squares) of (a) $Al_xIn_{1-x}P$ and (b) $AlAs_{1-x}P_x$ alloys compared with Vegard' spredi ction (dashed line).

Table 1.Calculated lattice parameter (a) and bulk modulus (B) for $Al_xIn_{1-x}P$ and $AlAs_{1-x}P_x$ alloys.

x	Lattice parameter a (Å)			Bulk modulus B (GPa)		
	Our work	Exp.	Other cal.	Our work	Exp.	Other cal.
$Al_xIn_{1-x}P$						
0	6.014	5.861[a]	5.93[a],5.942[c],5.968[d]	60.25	71[a]	76[a] ,73.26[c],62[d]
0.25	5.909			61.458		
0.5	5.792			65.575		
0.75	5.664			72.485		
1	5.534	5.47[b]	5.52[a],5.442[c],5.51[e],5.511[f],5.507[f]	81.89	86[b]	95.46[c],89[d],82.5[e],82.09[f],82.61[f]
$AlAs_{1-x}P_x$						
0	5.754	5.66[b]	5.74[e],5.731[f],5.726[f]	65.281	82[g]	66.8[e],67.73[f],68.27[f]
0.25	5.698			66.839		
0.5	5.641			71.456		
0.75	5.586			76.455		
1	5.534	5.47[b]	5.52[a],5.442[c],5.51[e],5.511[f],5.507[f]	81.89	86[b]	95.46[c],89[d],82.5[e],82.09[f],82.61[f]

[a]Ref.[17], [b]Ref.[18], [c]Ref.[19],[d]Ref.[20],[e]Ref.[21],[f]Ref.[22],

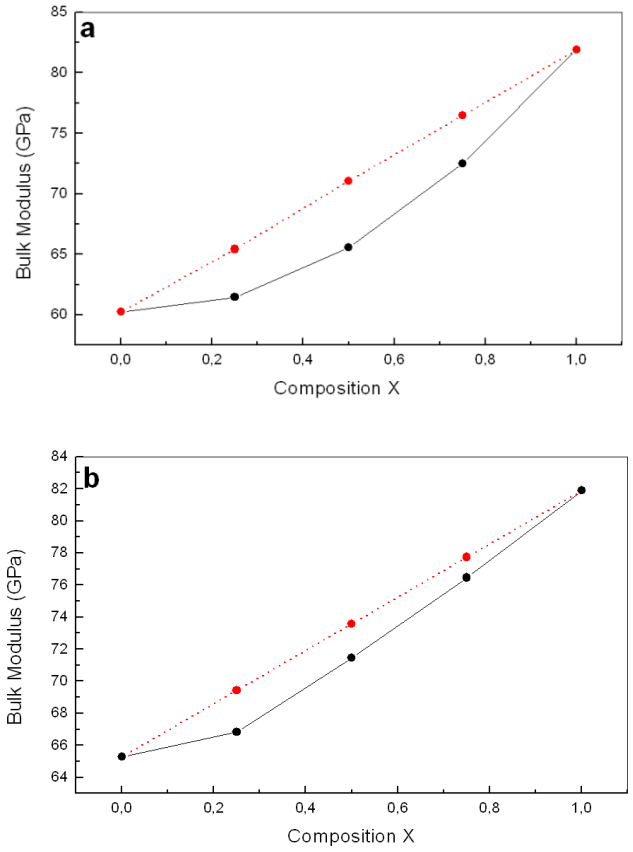

Fig. 2. Variation of the calculated bulk modulus versus x concentration of a) $Al_xIn_{1-x}P$ and (b) $AlAs_{1-x}P_x$ alloys (solid line) compared with LCD prediction (dashed line).

3.2. Electronic properties

The important features of the band structure (direct Γ-Γ and indirect Γ-X band gaps) are given in Table 2. It is clearly seen that the band gaps are on the whole underestimated in comparison with experiments results. This underestimation of the band gaps is mainly due to the fact that the GGA do note take into account the quasi-particle self energy correctly [23] which make them not sufficiently flexible to accurately reproduce both exchange and correlation energy and its charge derivative. We worth also mention that in general, it is far to say that the experimental data are well reproduced by the calculation. On raison for this difference is that in our calculations we have assumed the crystal to be at T = 0 K and thus do not include contributions from lattice vibrations that are present at room temperature measurements. The band structure calculations in the present work yield a direct gap (Γ-Γ) for InP, while for AlP and AlAs compounds an indirect gap (Γ-X) has been determined. Hence, one can expect that the band gap of Al*x*In1-*x*P and $AlAs_{1-x}P_x$ alloys should undergo a crossover between the direct and the indirect band in going from x = 0 to x = 1. As shown in Fig. 3, this crossover occurs atx = 0.82 for Al*x*In1-*x*P and we notice that for concentrations (x) ranging from x=0.03 to 0.85 the $AlAs_{1-x}P_x$ alloy exhibits a direct band gap (Γ→ Γ). The calculated band gap versus concentrations was fitted by a polynomial equation. The results are summarized as follows:

$$Al_xIn_{1-x}P \quad \begin{cases} E_{\Gamma-\Gamma} = 2.55 - 0.92x + 0.51\,x^2 \\ E_{\Gamma-X} = 1.89 + 3.71x - 3.90x^2 \end{cases} \qquad (1)$$

$$AlAs_{1-x}P_x \quad \begin{cases} E_{\Gamma-\Gamma} = 1.79 - 2.59x + 3.74\,x^2 \\ E_{\Gamma-X} = 1.51 + 5.62x - 5.45\,x^2 \end{cases} \qquad (2)$$

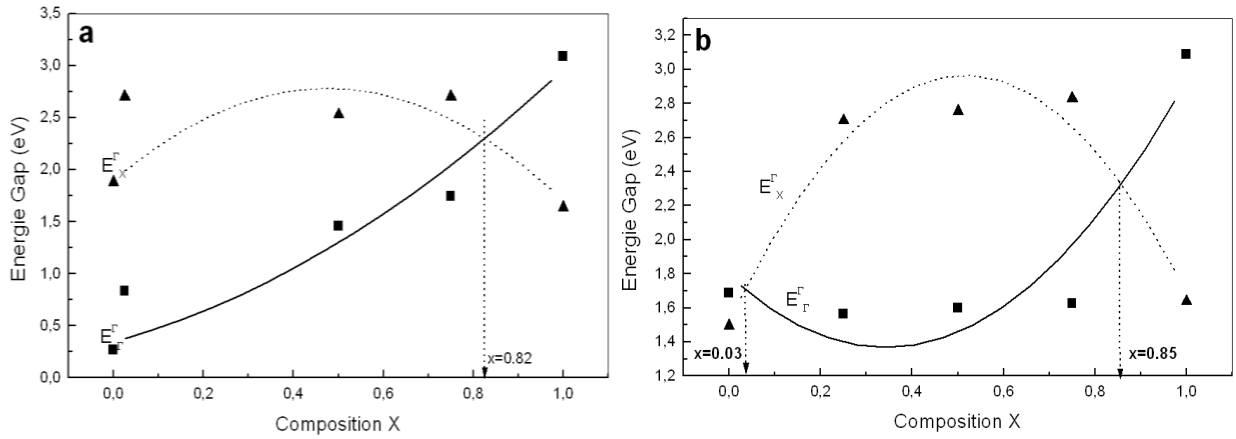

Fig. 3.Energy band gap of (a) $Al_xIn_{1-x}P$ and (b) $AlAs_{1-x}P_x$ alloys as a function of composition x.

Table 2.Gap energy Eg of $Al_xIn_{1-x}P$ and $AlAs_{1-x}P_x$ ternary alloys at equilibrium volume.

x	Energy gap (eV)(Γ-Γ)			Energy gap (eV)(Γ-X)		
	Our work	Exp.	Other cal.	Our work	Exp.	Other cal.
$Al_xIn_{1-x}P$						
0	0.267	1.39[a]	0.62[c] ,0.85[c]	1.880		1.552[h]
0.25	0.831			2.701		
0.5	1.457			2.527		
0.75	1.742			2.701		
1	3.088	3.63[e]	2.94[f], 3.083[g]	1.638	2.50[b]	1.57[c] , 1.635[d]
$AlAs_{1-x}P_x$						
0	1.688	3.13[e]	1.65[f], 1.787[g]	1.494	2.24[e]	1.43[f], 1.502[g]
0.25	1.563			2.699		
0.5	1.597			2.754		
0.75	1.624			2.830		
1	3.088	3.63[e]	2.94[f], 3.083[g]	1.638	2.50[b]	1.57[c] , 1.635[d]

[a]Ref.[26], [b]Ref.[27], [c]Ref.[28],[d]Ref.[29],[e]Ref.[30],[f]Ref.[21], [g]Ref.[22],[g]Ref.[47].

To understand the physical origins of the gap bowing parameter in $Al_xIn_{1-x}P$ and$AlAs_{1-x}P_x$ alloys, we follow the procedure of Bernard and Zunger [24]which decompose it into three contributions. Since the compositional effect on the bowing is considered to be small, the band gap bowing equations of Bernard and Zunger have been defined only by the contributions of the volume deformation (b_{VD}), charge transfer (b_{CT}) and the structural relaxation (b_{SR}) of the alloys as follows:

$$b = b_{VD} + b_{CT} + b_{SR} \quad (3)$$

The calculated gap bowing contributions of the direct band gap are presented in Table 3. The total gap bowing for Al_xIn_{1-x} P and$AlAs_{1-x}P_x$alloys has been found to be very small. The low value of b_{VD} is related to the weak mismatch of the lattice parameters of InP, AlP andAlP, AlAs compounds respectively and that of b_{CT} is due to the weak electronegativity [25] difference between In (1.78), As (2.18) and P (2.19) atoms. The small contribution of the structural relaxation to the bowing parameter it due to that our calculations are for ordered structure.

Table 3.Decomposition of optical bowing into volume deformation (VD), Charge exchange (CT), and structural relaxation (SR) contributions, all values are in eV.

x	Our work	Exp.	Other cal.
$Al_xIn_{1-x}P$			
b_{VD}	0.737		0.740[b]
b_{CT}	-0.090		0.265[b]
b_{SR}	0.233		-0.172[b]
b	0.880	0.568[a]	0.834[b]
$AlAs_{1-x}P_x$			
b_{VD}	1.494		-0.006[c],-0.01[c]
b_{CT}	1.563		0.064[c],0.038[c]
b_{SR}	1.597		-0.004[c],-0.008[c]
b	1.624		0.054[c],0.02[c],0.051[c],0.023[c]

[a]Ref.[31], [b]Ref.[32], [c]Ref.[22].

3.3. Linear optical properties

It is well known that the basic optical properties of semiconductors result from the electronic excitation in crystals when an electromagnetic wave is incident on them. The calculation of the optical properties of the solids is beset with numerous problems. The knowledge of the dielectric functions $\varepsilon(\omega) = \varepsilon_1(\omega) + i\varepsilon_2(\omega)$ allows to describe the optical properties of the medium at all phonon energies. Calculations of the dielectric function involve the energy eigenvalues and the electron wave functions. These are the natural output of the ab initio band structure calculation which is usually performed under GGA[33,34].We have calculated the frequency dependent imaginary dielectric function and real dielectric function. The effects of using K points in the BZ have already been discussed in the earlier work by Khan et al (1993)[35]. The knowledge of both the real and the imaginary parts of the dielectric function allows the calculation of important optical functions. In this paper, we also present and analyze the refractive index $\varepsilon(\omega)$ given by:

$$n(\omega) = \left[\frac{\varepsilon_1(\omega)}{2} + \frac{\sqrt{\varepsilon_1^2(\omega)+\varepsilon_2^2(\omega)}}{2}\right]^{1/2} \quad (4)$$

At low frequency ($\omega = 0$), we obtain the following relation:

$$n(0) = \varepsilon^{\frac{1}{2}}(0) \quad (5)$$

The refractive index and dielectric constants are very important to determine the optical and electric properties of the crystal. The use of these optical techniques for epitaxial layer characterization is limited by the accuracy with which refractive indices can be related to alloy composition. These applications require an analytical expression or known accuracy to relate the wavelength dependence of refractive index to alloy composition, as determined from simple techniques as photoluminescence. Different theoretical models relate the refractive index to the energy band gap for a large set of semiconductors [36-39]. Especially, for the III–V semiconductors and its alloys we take the most realistic model, proposed by Reedy and NazeerAhammed [39]:

$$n = \sqrt{\frac{12.417}{\sqrt{E_g - 0.365}}} \quad (6)$$

whereE_g is the energy gap in eV. This equation is a straightforward modification of the original Moss equation [37],with a second arbitrary constant (0.365) added in order to improve the results obtained.

Our results for InP, AlP and AlAs and their ternary alloys are listed in Table 4. It is clearly seen that the values of the refractive index obtained by FP-LMTO method are in reasonable agreement with the available data. In Fig. 4, we note that when x increases, n decreases as well. The refractive in dicesare related to their energy bands. There is a correlation between these two fundamental properties has a significant impact on the band structure of semiconductors [40].Given the fact that the Eg of the material of interest increases with increasing x (see Table 2) and n decreases with x (see Table 4). The calculated refractive indices versus concentration using FP- LMTO were fitted by a polynomial equation to find n equal to 0.508 and 0.251 for $Al_xIn_{1-x}P$ and $AlAs_{1-x}P_x$alloys, respectively. We can note the strong non-linear dependence of the refractive index of the alloys with concentration x. The results are summarized as follows:

$$Al_xIn_{1-x}P \begin{cases} n(x) = 2.552 - 0.926\,x + 0.508\,x^2 & \text{FP-LMTO} \\ n(x) = 3.814 - 3.537\,x + 5.522\,x^2 & \text{Reddy and al.} \end{cases} \quad (8)$$

$$AlAs_{1-x}P_x \begin{cases} n(x) = 2.324 - 0.449\,x - 0.251\,x^2 & \text{FP-LMTO} \\ n(x) = 3.414 - 0.161\,x + 0.064\,x^2 & \text{Reddy and al.} \end{cases} \quad (10)$$

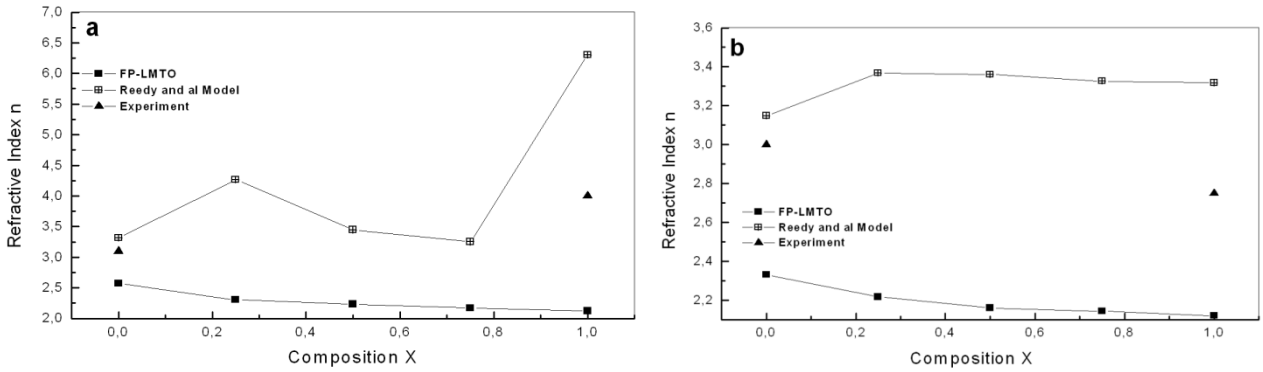

Fig. 4. Variation of the calculated refractive index versus x concentration of (a) $Al_xIn_{1-x}P$ and (b) $AlAs_{1-x}P_x$ alloys.

Table 4. Refractive indices of $Al_xIn_{1-x}P$ and $AlAs_{1-x}P_x$ for different compositions x.

x	This work		Exp.	Other cal.
	FP-LMTO	Reedy model		
$Al_xIn_{1-x}P$				
0	2.574	3.317	3.098[a]	2.814[c]
0.25	2.305	4.263		
0.5	2.232	3.447		
0.75	2.170	3.252		
1	2.119	6.304	4.0[b]	2.372[c]
$AlAs_{1-x}P_x$				
0	2.330	3.148	3.00[d]	2.833[e],2.969[e]
0.25	2.216	3.368		2.757[e],2.955[e]
0.5	2.160	3.360		2.715[e],2.934[e]
0.75	2.142	3.326		2.671[e],2.911[e]
1	2.119	3.317	2.75[d]	2.651[e],2.892[e]

[a]Ref.[41], [b]Ref.[27], [c]Ref.[42],[d]Ref.[43],[e]Ref.[22]

3.4. Thermodynamic properties

In order to study the phase stability of $Al_xIn_{1-x}P$ and $AlAs_{1-x}P_x$alloys the Gibbs free energy of mixing $\Delta G_m(x, T)$ is calculated in order to access the T–x phase diagram and obtain the critical temperature, Tc, for miscibility. More details of the calculations are given in Refs.[44–46]. The Gibbs free energy of mixing, ΔG_m, for alloys can be expressed by:

$$\Delta G_m = \Delta H_m - T\Delta S_m \quad (11)$$

where

$$\Delta H_m = \Omega x(1-x) \quad (12)$$

$$\Delta S_m = -R[x\ln x + (1-x)\ln(1-x)] \quad (13)$$

ΔHm and ΔSm are the enthalpy and entropy of mixing, respectively; Ω the interaction parameter and depends on material; R the perfect gas constant and T the absolute temperature. The mixing enthalpy of alloys can be obtained from the calculated total energies as:

$$\Delta H_m = E_{AB1-xCx} - (1-x)E_{AB} - xE_{AC},$$

where $E_{AB1-xCx}$, E_{AB}, and E_{AC} are the respective energies of AB_xC_{1-x} alloy and the binary compounds AB, and AC. We then calculated ΔH_m to obtain Ω as a function of concentration. The interaction parameter increases almost linearly with increasing x. From a linear fit we obtained:

$$Al_xIn_{1-x}P \longrightarrow \Omega(\text{Kcal/mol}) = 34.6733 + 2.1126x$$
$$AlAs_{1-x}P_x \longrightarrow \Omega(\text{Kcal/mol}) = 1.9326 + 0.4594x$$

The average values of the x-dependent Ω in the range $0 < x < 1$ derived from these equations for $Al_xIn_{1-x}P$ and $AlAs_{1-x}P_x$alloys are 35.7296 and 2.1623 kcal/mol, respectively. The larger enthalpy for $Al_xIn_{1-x}P$alloy suggests a large value of Ω and, hence a higher critical temperature.

By calculating the temperature composition phase diagram which shows the stable, metastable, and unstable mixing regions of the alloy. At a temperature lower than the critical temperature T_c, the two binodal points are determined as those points at which the common tangent line touches the ΔG_m curves. The two spinodal points are determined as those points at which the second derivative of ΔG_m is zero. The spinodal and binodal curves of the alloys shown in Fig. 5.

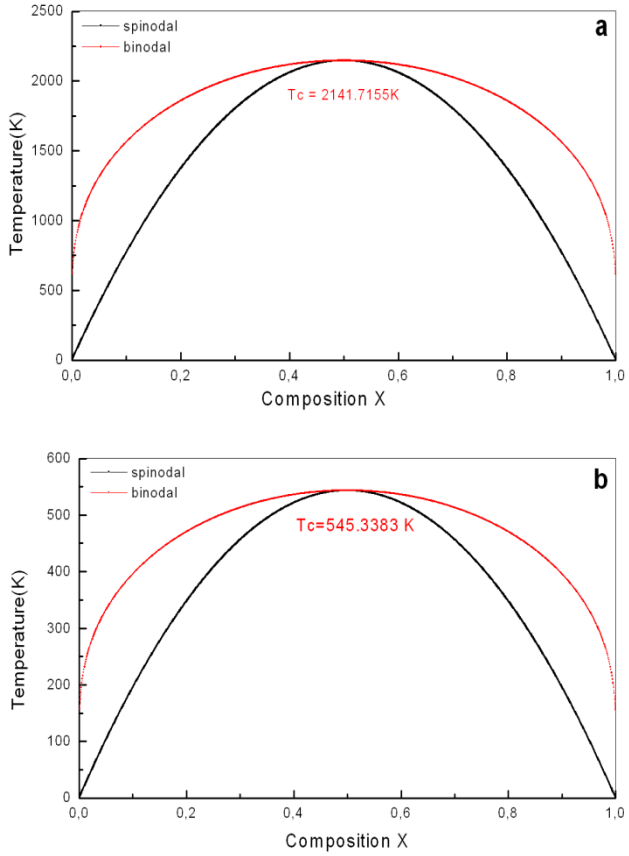

Fig. 5. T–x phase diagram for (a) $Al_xIn_{1-x}P$ and (b) $AlAs_{1-x}P_x$ alloys. Black line: binodal curve, Red line: spinodal curve.

We have calculated the phase diagram by using the average values of the x-dependent Ω, hence the phase diagram looks symmetric. In Fig. 4, we observed a critical temperature T_c of 2141.7155 and 545.3383 K for $Al_xIn_{1-x}P$ and $AlAs_{1-x}P_x$ alloys, respectively. The spinodal curve in the phase diagram marks the equilibrium solubility limit, i.e. the miscibility gap. A homogeneous alloy is predicted for temperatures and compositions above this curve. The wide range between spinodal and bimodal curves indicates that the alloy may exist as a metastable phase. Finally, our results indicate that the $AlAs_{1-x}P_x$alloy is stable at low temperature while the $Al_xIn_{1-x}P$is stable at high temperature.

4. Conclusions

In summary, a theoretical investigation of the structural, electronic, optical and thermodynamic properties of ternary mixed crystals $Al_xIn_{1-x}P$ and $AlAs_{1-x}P_x$has been reported. The agreement between our results and the available experimental and theoretical data is found to be generally satisfactory. We have investigated the composition dependence of the lattice constant, bulk modulus, band gap, refractive index and dielectric function. A small deviation of the lattice constant from Vegard's law was observed for $Al_xIn_{1-x}P$, while the lattice parameter at different compositions for $AlAs_{1-x}P_x$was found to vary almost linearly, thus obeying Vegard's law. This is mainly because of the large mismatch of the lattice parameters of the binary compounds InP and AlP. A non-linear dependence on the composition x was observed for the bulk modulus of the two alloys. The gap bowing is mainly caused by the charge-transfer effect, while the volume deformation and the structural relaxation contribute at smaller magnitude for the two alloys.

Using FP-LMTO method and Reddy and al the refractive index has been calculated as a function of composition x. Our results showed that the refractive index varies none linearly with respect to x exhibiting different bowing parameters which arise from the effects of compositional alloy disorder.

The investigation of the thermodynamic stability allowed us to calculate the critical temperatures for $Al_xIn_{1-x}P$ and $AlAs_{1-x}P_x$alloys, which are 2141.7155 and 545.3383 K respectively.

References

[1] I. Vurgaftman, J. R. Meyer, L. R. Ram-Mohan, J. Appl. Phys. **89**, 5815 (2001).
[2] S. Adachi, World Scientific, Singapore, 1994.
[3] T. Ohnuma, M. Nagano, Jpn. J. Appl. Phys. **39**, L972 (2000).
[4] (a) M.-Z. Huang, W. Y. Ching, Phys. Rev. B **47**, 9449 (1993); (b) M.-Z. Huang, W. Y. Ching, Phys. Rev. B **47**, 9464 (1993).
[5] A. R. Jivani, H. J. Trivedi, P. N. Gajjar, A. R. Jani, Pramana J. Phys. **64**(1), 153 (2005).
[6] S. Zh. Karaahanov, L. C. Yan Voon, Semiconductors **39**(2), 161 (2005).
[7] J. P. Perdew, Y. Wang, Phys. Rev. B **45**, 13244 (1992).
[8] (a) G. P. Srivastava, G. L. Martins, A. Zunger, Phys. Rev. B **31**, 2561 (1985); 2561 (1985); (b) J.E. Bernard, A. Zunger, Phys. Rev. B **34**, 5992 (1986).
[9] S. Y. Savrasov, Phys. Rev. B **54**, 16470 (1996).
[10] S. Savrasov, D. Savrasov, Phys. Rev. B **46**, 12181 (1992).
[11] D. Rached, M. Rabah, N. Benkhettou, M. Driz, B. SoudiniPhysica B: Physics of Condensed Matter, **337**(1-4), 394(2003).
[12] J. P. Perdew, S. Burke, M. Ernzerhof, Phys. Rev. Lett. **77**, 3865 (1996).

[13] P. Blochl, O. Jepsen, O. K. Andersen, Phys. Rev. B **49**, 16223 (1994).
[14] F. D. Murnaghan, Proc. Natl. Acad. Sci. USA **30**,244 (1944).
[15] A. Mokhtari, H. Akbarzadeh, Physica B **324**,305 (2002).
[16] L. Vegard, Z. Phys. **5**, 17 (1921).
[17] O. Madelung, L. Bornstein, **17**, New Series, Group III, Springer Verlag, Berlin, 1982.
[18] K.-H. Hellwege, O. Madelung (Eds.), Semi-Conductor, Intrinsic Properties of Group IV Elements and III_V, II_VI and I_VII Compounds, Landolt-Bornstein New Series, Group III, vol. **22**, Pt Springer, Berlin, 1982.
[19] V. Khanin, S. E. Kul'kova, Russian Physics Journal, **48**(1), 61 (2005).
[20] I. Vurgaftman, J. R. Meyer, L. R. Ram-Mohan, Journal of Applied Physics, **89**(11), 5815 (2001).
[21] M. Briki, M. Abdelouhaba, A. Zaoui, M. Ferhat, Superlatt.Microstruct.**45**,80 (2009).
[22] F. Annane, H. Meradji, S. Ghemid, F. El Haj Hassan, Computational Materials Science **50**,274 (2010).
[23] S. N. Rashkeev, W. R. L. Lambrecht, Physical Review. B, **63**(16), 165212 (2001).
[24] (a) G. P. Srivastava, G. L. Martins, A. Zunger, Phys. Rev. B **31**, 2561 (1985); (b) J. E. Bernard, A. Zunger, Phys. Rev. B **34**, 5992 (1986).
[25] W. Sargent, Table of Periodic Properties of the Elements, Sargent-Welch Scientific, Skokie, IL, 1980.
[26] E. Brustein, H. Brodsky, G. Lucousky, International Journal of Quantum Chemistry, **756**, 1987. Communications, **135**(1-2), 124 (2005).
[30] M. P. Thompson, G. W. Auner, T. S. Zheleva, K. A. Jones, S. J. Simko, J. N. Hilfiker, J. Appl. Phys. **89**, 3321 (2001).
[27] W. A. Harrison, Freeman, San Francisco, 1980.
[28] R. Ahmed, Fazal-e-Aleem, S. J. Hashemifar, H. Akbarzadeh, PhysicaB,**403**(10-11), 1876 (2008).
[29] L. H. Yu, K. L. Yao, Z. L. Liu, Solid State
[31] M. Moser, R. Wienterhoff, C. Geng, J. Quisser, F. Scholz, A. Dörden, Applied Physics Letters, **64**(2), 235 (1994).
[32] M. Ferhat, Physica Status Solidi (B), **241**(10), R38 (2004).
[33] M. Alouani, J. M. Koch, M. A. Khan, J. Phys. **F16**, 437 (1986).
[34] C. Koenig, M. A. Khan, Phys. Rev. **B17**, 6129 (1983).
[35] M. A. Khan, A. Kashyap, A. K. Solanki, T. Nautiyal, Auluck S Phys. Rev. **B48**, 16947 (1993).
[36] Y. Al Douri, H. Abid, H. Aourag, Mater. Chem. Phys. **65**, 117 (2000).
[37] T. S. Moss, Phys. Status Solidi (b) **131**, 415 (1985).
[38] N. M. Ravindra, S. Anuch, V. K. Srinvastava, Phys. State Solid (b) **93**,115 (1979).
[39] R. Reddy, Y. NazeerAhammed, Infra. Phys. Technol. **36**,825 (1995).
[40] N. M. Ravindra, P. Ganapathy, J. Choi, Infrared Phys. Technol. **50**, 21 (2007).
[41] E. Burstein, H. Brodsky, G. Lucousky, Int. J. Opt. Soc. Am. **47**, 240 (1957).
[42] Ming-Zhu Huang, W. Y. Ching, Phys. Rev. B, **31**, N.15 (1993).
[43] R. R. Reedy et al., J. Alloys Compd. **473**, 28 (2009).
[44] R. A. Swalin, Thermodynamics of Solids, Wiley, New York, 1961.
[45] L. G. Ferreira, S. H. Wei, J. E. Bernard, A. Zunger, Phys. Rev. B **40**, 3197 (1999).
[46] L. K. Teles, J. Furthmuller, L. M. R. Scolfaro, J. R. Leite, F. Bechstedt, Phys. Rev. B **62**, 2475 (2000).
[47] S. Z. Karazhanov, L. C. Lew Yan Voon, Semiconductors, **39**(2), 161 (2005).

*Corresponding author: lilo.btf@gmail.com